Anisotropy induced vortex lattice rearrangement in CaKFe_{4}As_{4}

Rustem Khasanov, William R. Meier, Sergey L. Bud'ko, Hubertus Luetkens, Paul C. Canfield, and Alex Amato

Anisotropy induced vortex lattice rearrangement in CaKFe$_4$As$_4$

Rustem Khasanov,[1, *] William R. Meier,[2, 3] Sergey L. Bud'ko,[2, 3]
Hubertus Luetkens,[1] Paul C. Canfield,[2, 3] and Alex Amato[1]

[1]*Laboratory for Muon Spin Spectroscopy, Paul Scherrer Institut, CH-5232 Villigen PSI, Switzerland*
[2]*Division of Materials Science and Engineering, Ames Laboratory, Ames, Iowa 50011, USA*
[3]*Department of Physics and Astronomy, Iowa State University, Ames, Iowa 50011, USA*

The magnetic penetration depth anisotropy $\gamma_\lambda = \lambda_c/\lambda_{ab}$ (λ_{ab} and λ_c are the in-plane and the out-of-plane components of the magnetic penetration depth) in a CaKFe$_4$As$_4$ single crystal sample (the critical temperature $T_c \simeq 35$ K) was studied by means of muon-spin rotation (μSR). γ_λ is almost temperature independent for $T \lesssim 20$ K ($\gamma_\lambda \simeq 1.9$) and it reaches $\simeq 3.0$ by approaching T_c. The change of γ_λ induces the corresponding rearrangement of the flux line lattice (FLL), which is clearly detected via enhanced distortions of the FLL μSR response. Comparison of γ_λ with the anisotropy of the upper critical field ($\gamma_{H_{c2}}$) studied in Phys. Rev B **94**, 064501 (2016), reveals that γ_λ is systematically higher than $\gamma_{H_{c2}}$ at low-temperatures and approaches $\gamma_{H_{c2}}$ for $T \to T_c$. The anisotropic properties of λ are explained by the multi-gap nature of superconductivity in CaKFe$_4$As$_4$ and are caused by anisotropic contributions of various bands to the in-plane and the out-of-plane components of the superfluid density.

In the majority of superconducting compounds discovered so far, the crystal structure, as well as the electronic and phononic band structures are all far from being isotropic. Anisotropic superconductors are usually treated within the phenomenological anisotropic Ginzburg-Landau (AGL) theory,[1,2] which follows from the isotropic Ginzburg-Landau (GL) approach via replacement of the effective mass m^* in the GL free energy functional by an effective mass tensor, with values m_a^*, m_b^*, and m_c^* along the principal $a-$, $b-$, and $c-$axes.[3,4] In the most usual case of uniaxial anisotropy, all anisotropies are incorporated into the single parameter:[5]

$$\gamma = \gamma_\lambda \equiv \frac{\lambda_c}{\lambda_{ab}} = \sqrt{\frac{m_c^*}{m_{ab}^*}} = \gamma_{H_{c2}} \equiv \frac{H_{c2}^{\|ab}}{H_{c2}^{\|c}} = \frac{\xi_{ab}}{\xi_c}. \quad (1)$$

Here γ_λ and $\gamma_{H_{c2}}$ are the anisotropy of the magnetic penetration depth (λ) and the upper critical field (H_{c2}), respectively, and ξ is the coherence length. In AGL theory the same effective mass tensor determines the anisotropy of λ and H_{c2}, thus making both γ_λ and $\gamma_{H_{c2}}$ temperature and field independent.[6]

Note, however, that the GL theory is strictly valid only for $T \to T_c$. Following Kogan,[7] away from T_c the theoretical approach for calculating H_{c2} (the position of the second order phase transition in high fields) has little in common with evaluation of λ, so that the anisotropies γ_λ and $\gamma_{H_{c2}}$ are not the same and can be substantially different. In MgB$_2$, *e.g.*, both anisotropies approach a common value $\gamma_\lambda = \gamma_{H_{c2}} \simeq 1.75$ at T_c and become $\gamma_\lambda \simeq 1.2$ and $\gamma_{H_{c2}} \simeq 6$ at low temperatures.[8–10] Different T dependencies of γ_λ and $\gamma_{H_{c2}}$ have also been reported for various cuprate and Fe-based superconductors.[11–19]

It is worth to mention here, that the change of γ_λ would necessarily lead to a corresponding flux line lattice (FLL) rearrangement. As follows from Fig. 1 (a), for the external field B_{ex} applied along the $ab-$plane ($B_{ex} \parallel ab$), the increase of γ_λ shortens the distance between vortices within the ab plane and enhances the intervortex

distances in the $c-$direction. The displacement of vortex lines could be quite big. The simple estimate reveals that the increase of γ_λ from 1.0 to 3.0 leads to decrease/increase of the in-plane/out-of-plane intervortex distances by almost half of the isotropic FLL unit cell [see Fig. 1 (a)]. This effect can be studied, *e.g.* by using techniques visualizing the vortex distribution in superconducting materials, such as small-angle neutron scattering (SANS), tunneling or magnetic decoration. The important limitation comes, however, from the sample size and morphology. Most of the available good quality single crystals are very thin along the crystallographic $c-$direction, as well as a good surface preparation (needed for magnetic decoration and tunneling experiments) in $B_{ex} \perp c$ orientation is challenging.

In this paper, we report on measurements of the magnetic penetration depth anisotropy $\gamma_\lambda = \lambda_c/\lambda_{ab}$ in a CaKFe$_4$As$_4$ single crystal sample ($T_c \simeq 35$ K) by means of the muon-spin rotation (μSR). Comparison of γ_λ with $\gamma_{H_{c2}}$ studied in Ref. 21 shows that γ_λ is higher than $\gamma_{H_{c2}}$ all the way up to T_c. Only in the narrow region close T_c, $\gamma_\lambda = \gamma_{H_{c2}} \simeq 3.0$ [Fig. 1 (b)]. The change of γ_λ with temperature induces the corresponding rearrangement of the flux line order, which was detected via the enhanced distortions of FLL μSR response. The temperature dependencies of the in-plane and the out-of-plane components of the superfluid density (λ_{ab}^{-2} and λ_c^{-2}) were found to be well described within the two-gap scenario, thus suggesting that the multiple-band nature of superconductivity in CaKFe$_4$As$_4$ is well pronounced for both $c-$ and $ab-$ directions.

CaKFe$_4$As$_4$ single crystal with dimensions of $\simeq 4.0 \times 4.0 \times 0.1$ mm^3 was grown from a high-temperature Fe-As rich melt,[21,22] and it is characterized via magnetization measurements (see the Supplemental part, Ref. 20). The μSR measurement were carried out at the πM3 beam line using the GPS spectrometer (Paul Scherrer Institute, Switzerland).[23] The zero-field (ZF) and transverse-field (TF) μSR measurements were performed at temper-
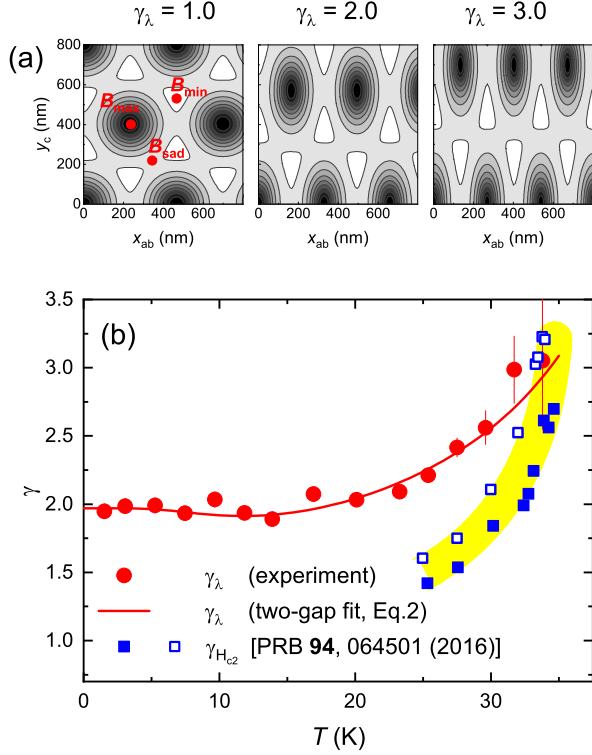
FIG. 1: (a) The contour plot of the field variation within the triangular vortex lattice of anisotropic superconductor with $B_{ex} \parallel ab$ ($B_{ex} = 11$ mT, $\gamma_\lambda = \lambda_c/\lambda_{ab} = 1.0$, 2.0, and 3.0; see the Supplemental part, Ref. 20). B_{min}, B_{max}, and B_{sad} are the minimum, maximum and the saddle point fields. (b) The anisotropies γ_λ and $\gamma_{H_{c2}}$ of CaKFe$_4$As$_4$. Closed circles are γ_λ points from the present study. The closed and open squares correspond to $\gamma_{H_{c2}}(T)$ from Ref. 21, as obtained by using the 'onset' and 'offset' criteria of T_c determination, respectively. The solid red line is the fit of two-gap model (Eq. 2) to $\lambda_{ab}^{-2}(T)$ and $\lambda_c^{-2}(T)$ data.

FIG. 2: The Fast Fourier transform of the TF-μSR time spectra. Panels (a)–(c) correspond to $B_{ex} \parallel ab$ and panels (e)–(f) to $B_{ex} \parallel c$ set of measurements, respectively.[27] The solid and open red symbols are $P(B)$'s obtained by following FCW and FCC protocols at $B_{ex} \simeq 10.8$ mT (see text for details). The blue closed symbols are $P(B)$'s after the field shift down to $\simeq 8$ mT. Dashed lines correspond to the applied field (10.8 mT) and to the 'shifted' field (8.0 mT), respectively.

atures from $\simeq 1.5$ to 50 K. In two sets of TF-μSR experiments the external magnetic field ($B_{ex} \simeq 10.8$ mT) was applied parallel to the $ab-$plane and the crystallographic $c-$axis of the crystal, respectively. A fraction of TF-μSR data for $B_{ex} \parallel c$ was previously reported in Ref. 24. ZF-μSR data are discussed in the Supplemental part, Ref. 20. A special sample holder designed to measure thin samples by means of μSR was used.[25] The experimental data were analyzed using the MUSRFIT package.[26]

The homogeneity of the superconducting state in CaKFe$_4$As$_4$ was checked by performing series of field-shift experiments. Figure 2 exhibits the Fast Fourier transform of the TF-μSR time spectra, which reflects the internal field distribution $P(B)$. The panels (a) to (c) corresponds to $B_{ex} \parallel ab$ and panels (e) to (f) to $B_{ex} \parallel c$ set of measurements, respectively. The solid red symbols are $P(B)$'s obtained after cooling the sample at $B_{ex} = 10.8$ mT from a temperature above T_c down to 1.48 K and subsequent warming it up to the measurement temperature [field-cooled warming (FCW) proce-
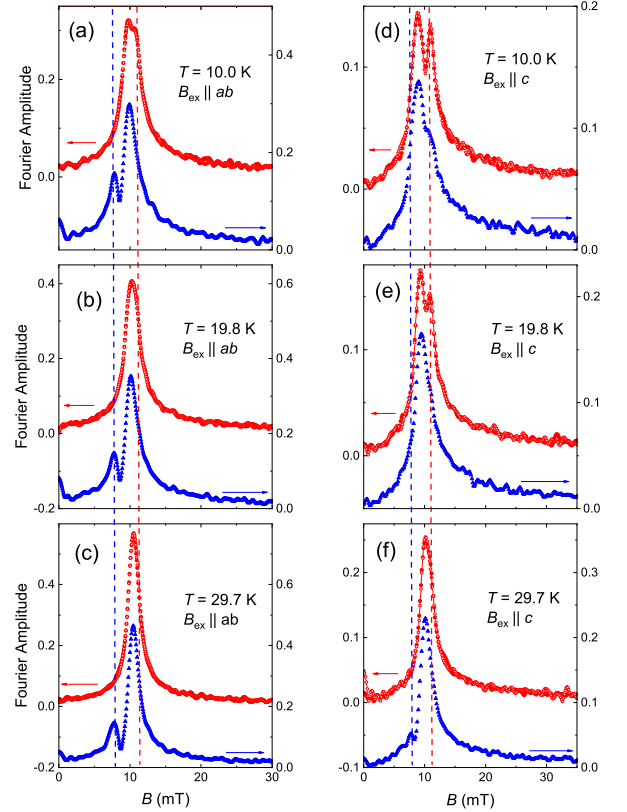
dure]. The open red symbols are $P(B)$'s obtained after direct cooling from $T > T_c$ to the measurement temperature [field-cooled cooling (FCC) procedure]. The blue closed symbols are $P(B)$'s distributions collected by following the FCW protocol and subsequent decrease of the external field down to $\simeq 8$ mT (field-shift procedure). From the data presented in Fig. 2 the following three important points emerges. (i) The main part of the signal, accounting for approximately 90% of the total signal amplitude, remains unchanged within the experimental error after a field shift. Only the sharp peak ($\simeq 10\%$ of the signal amplitude) follows exactly the applied field. It is attributed, therefore, to the residual background signal from muons missing the sample (see also Refs. 25,28). (ii) The asymmetric $P(B)$ distributions shown in Fig. 2 possess the basic features expected for a well aligned vortex lattice, i.e., the cutoff at low fields (B_{min}), the peak arising from the saddle point midway between two adjacent vortices (B_{sad}), and a long tail towards high fields caused by regions around the vortex core (B_{max}).[24;29] Note that the definition of "well

aligned" FLL is different, *e.g*, for μSR and SANS experiments. In μSR case, due to the microscopic nature of μSR technique, the field at the muon stopping site is determined by the *local* flux line arrangement (within a couple of FLL unit cells). SANS experiment collects reflections from flux-line planes, which requires a *long range* arrangement of FLL. Following scanning tunneling microscopy (STM) results, the FLL in $CaKFe_4As_4$ is well arranged on the short length scale, while the long range arrangement is missing [see Figs. 3 (d), (e), and (f) in Ref. 30]. (iii) The $P(B)$ curves obtained by following the FCC and FCW protocols coincide for both field orientations and within the full temperature range studied. To conclude, the above experiment demonstrates that the FLL in $CaKFe_4As_4$ sample is well arranged and strongly pinned (at least at $B_{ex} \simeq 11$ mT). The strong pinning in $CaKFe_4As_4$ was also reported for $B_{ex} \parallel c$ orientation in STM experiments,[30] and for both $B_{ex} \parallel ab$ and $B_{ex} \parallel c$ set of data in magnetization studies.[31]
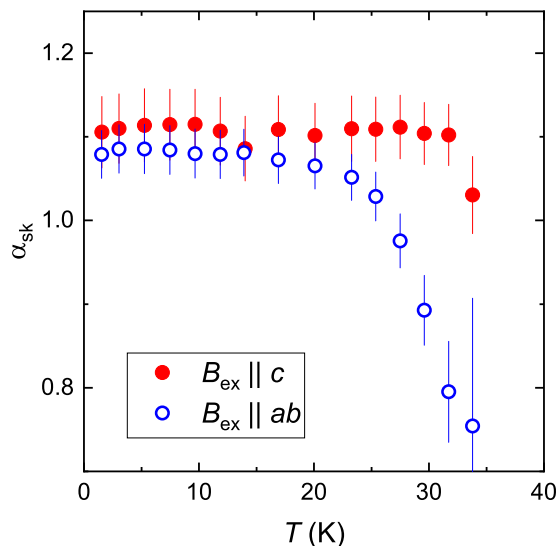

FIG. 3: The temperature dependence of the skewness parameter $\alpha_{sk} = \langle \Delta B^3 \rangle^{1/3} / \langle \Delta B^2 \rangle_s^{1/2}$ obtained in $B_{ex} \parallel c$ and $B_{ex} \parallel ab$ set of experiments.

The TF-μSR data were analyzed by fitting a three-component expression to the time evolution of the muon-spin polarization (see the Supplemental part, Ref. 20). The superconducting response of $CaKFe_4As_4$ sample was further obtained within the framework of the so-called momentum approach, which includes the calculations of the first moment ($\langle B \rangle$), and the second- ($\langle \Delta B^2 \rangle$) and third-central moments ($\langle \Delta B^3 \rangle$) of the magnetic field distribution function $P(B)$ (see the Supplemental part, Ref. 20, for details). Following Ref. 32, the first moment (the mean field) scales with the sample magnetization. The second moment (the broadening of the signal), $\langle \Delta B^2 \rangle = \langle \Delta B^2 \rangle_s + \sigma_{nm}^2$, contains contributions from the vortex lattice ($\langle \Delta B^2 \rangle_s$) and the nuclear dipole field [σ_{nm},

as is obtained from $T > T_c$ measurements]. In extreme type-II superconductors ($\lambda \gg \xi$) and for fields $B_{ex} \ll \mu_0 H_{c2}$, $\langle \Delta B^2 \rangle_s \propto \lambda^{-4}$.[33,34] The third moment accounts for the asymmetric shape of $P(B)$, which is described via the skewness parameter $\alpha_{sk} = \langle \Delta B^3 \rangle^{1/3} / \langle \Delta B^2 \rangle_s^{1/2}$. In the limit of $\lambda \gg \xi$ and for realistic measurement conditions $\alpha_{sk} \simeq 1.2$, for a well arranged triangular vortex lattice.[35] It is very sensitive to structural changes of the vortex lattice which may occur as a function of temperature and/or magnetic field.[35–40]

Figure 3 shows temperature dependencies of the skewness parameter α_{sk} measured in $B_{ex} \parallel c$ ($\alpha_{sk}^{\parallel c}$) and $B_{ex} \parallel ab$ ($\alpha_{sk}^{\parallel ab}$) set of experiments. The temperature dependencies of the first moment $\langle B \rangle$ and the second-central moment $\langle \Delta B^2 \rangle$ are presented in the Supplemental part.[20] Following Fig. 3, $\alpha_{sk}^{\parallel c}$ stays temperature independent. Only in the close vicinity to T_c, $\alpha_{sk}^{\parallel c}$ decreases by approximately 8% (from $\simeq 1.1$ to $\simeq 1.03$). This, together with the relatively high value of $\alpha_{sk}^{\parallel c} \simeq 1.1$ suggests, that in $B_{ex} \parallel c$ orientation the FLL in $CaKFe_4As_4$ is well developed and has little distortions. The presence of well arranged FLL is also confirmed in 'field-shift' experiments [Figs. 2 (d)–(f)] showing asymmetric $P(B)$'s with all characteristic features attributed to FLL.

The temperature evolution of $\alpha_{sk}^{\parallel ab}$ is, however, different from $\alpha_{sk}^{\parallel c}(T)$, Fig. 3. By increasing temperature, $\alpha_{sk}^{\parallel ab}$ stays almost constant up to $T \simeq 20$ K ($\alpha_{sk}^{\parallel ab} \simeq 1.07$) and it decreases down to $\simeq 0.7$ by approaching T_c. In general, the change of α_{sk} as a function of magnetic field and temperature is associated with the vortex lattice melting,[36,37,40] and/or dimensional crossover from 3D to 2D type of FLL.[35,37] Both processes are thermally activated and caused by increased vortex mobility via loosing the interplanar or intrapalanar FLL correlations.[37] In both interpretations, however, the increased vortex mobility leads to decoupling vortices from the pinning centers. This is not the case for $CaKFe_4As_4$ studied here. The 'field-shift' experiments, in $B_{ex} \parallel ab$ orientation, suggest of the FLL remaining rigid [at least up to $T \simeq 32$ K, see Fig. 2 (a)–(c) and the Supplemental part, Ref. 20]. This, therefore, rather indicates that the decrease of $\alpha_{sk}^{\parallel ab}$ for $T \gtrsim 20$ K is caused by γ_λ induced rearrangement of the FLL. The change of γ_λ, leading necessarily to the movement of the vortex lines [Fig. 1 (a)], enhances the pinning caused FLL distortions and, as a consequence, reduces the value of the skewness parameter $\alpha_{sk}^{\parallel c}$.

The T dependence of γ_λ was further studied via measurements of temperature evolutions of the in-plane (λ_{ab}^{-2}) and the out-of-plane (λ_c^{-2}) superfluid density components (Fig. 4). The anisotropy parameter $\gamma_\lambda = \lambda_c / \lambda_{ab}$ is presented in Fig. 1 (b). Obviously, γ_λ in $CaKFe_4As_4$ is temperature dependent. It is almost constat ($\gamma_\lambda \simeq 1.9$) for $T \lesssim 20$ K and increases up to $\simeq 3.0$ by approaching T_c. More remarkable is that $\gamma_\lambda(T)$ follows the temperature evolution of the skewness parameter $\alpha_{sk}^{\parallel ab}$. Both,
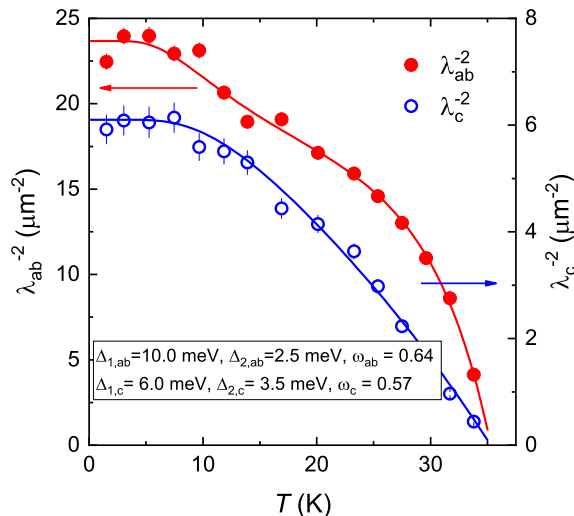
FIG. 4: Temperature dependencies of the inverse squared in-plane (λ_{ab}^{-2}) and the out-of-plane (λ_c^{-2}) components of the magnetic field penetration depth. Solid lines are fits within the framework of the phenomenological α−model.[12,41]

$\gamma_\lambda(T)$ and $\alpha_{\mathrm{sk}}^{\|ab}$ are *constant* for $T \lesssim 20$ K and change almost linearly in 25 K $\lesssim T < T_c$ region [Figs. 1 (b) and 3]. These suggest, that the enhancement of FLL distortions, seen via decrease of $\alpha_{\mathrm{sk}}^{\|ab}$ (Fig. 3) is caused by the vortex lattice rearrangement [Fig. 1 (a)], which, in its turn, is initiated by the temperature dependent anisotropy coefficient γ_λ [Fig. 1 (b)].

The comparison of γ_λ obtained in or study with $\gamma_{H_{c2}}$ reported in Ref. 21 shows that these anisotropies coincide with the each other ($\gamma_\lambda = \gamma_{H_{c2}} \simeq 3.0$) only for $T \to T_c$ [Fig. 1 (b)], thus resembling the situation in the famous two-gap superconductor MgB$_2$.[8–10] This may suggest that, the range of applicability of AGL to CaKFe$_4$As$_4$ is confined within a narrow range close to T_c, in full analogy with MgB$_2$, where the AGL description was found to be limited to temperatures less than 2% away from T_c.[42] An alternative approach, based on microscopic Eilenberger calculations, reveals that in two-gap superconductors (as *e.g.* MgB$_2$) γ_λ and $\gamma_{H_{c2}}$ have different temperature dependencies and cross only at T_c.[43] Which of these approaches better describe the anisotropic properties of CaKFe$_4$As$_4$ need further investigation.

The temperature dependencies of λ_{ab}^{-2} and λ_c^{-2} (Fig. 4) were further analyzed within the framework of the phenomenological α−model by decomposing $\lambda^{-2}(T)$ into two components:[12,41,44]

$$\frac{\lambda^{-2}(T)}{\lambda^{-2}(0)} = \omega \, \frac{\lambda^{-2}(T, \Delta_1)}{\lambda^{-2}(0, \Delta_1)} + (1-\omega) \, \frac{\lambda^{-2}(T, \Delta_2)}{\lambda^{-2}(0, \Delta_2)}. \quad (2)$$

Here $\lambda(0)$ is the value of the penetration depth at $T = 0$, Δ_i is the zero-temperature value of i−th gap ($i = 1$ or 2) and ω ($0 \leq \omega \leq 1$) is the weight

of the larger gap to λ^{-2}. Each component in Eq. 2 was further evaluated by $\lambda^{-2}(T, \Delta)/\lambda^{-2}(0, \Delta) = 1 + 2 \int_{\Delta(T)}^{\infty} (\partial f/\partial E) E/\sqrt{E^2 - \Delta(T)^2} \, dE$.[5] Here $f = [1 + \exp(E/k_B T)]^{-1}$ is the Fermi function and $\Delta(T) = \tanh\{1.82[1.018(1/t - 1)]^{0.51}\}$.[41] Note that this equation is valid within the clean-limit, which is indeed the case for CaKFe$_4$As$_4$.[21] Solid lines in Fig. 4 are fits of Eq. 2 to $\lambda_{ab}^{-2}(T)$ and $\lambda_c^{-2}(T)$ data. The fit parameters are: $\lambda_{ab}^{-2}(0) = 23.4$ (μm^{-2}), $\Delta_{1,ab} = 10.0$ meV, $\Delta_{2,ab} = 2.5$ mev $\omega_{ab} = 0.64$, and $\lambda_c^{-2}(0) = 6.1$ (μm^{-2}), $\Delta_{1,c} = 6.0$ meV, $\Delta_{2,c} = 3.5$ meV, $\omega_c = 0.57$ for $\lambda_{ab}^{-2}(T)$ and $\lambda_c^{-2}(T)$ data sets, respectively.

From the results of two-gap model fit to $\lambda_{ab}^{-2}(T)$ and $\lambda_c^{-2}(T)$, three important points emerge: (i) The 'theoretical' two-gap $\gamma_\lambda(T)$ curve stays in a good agreement with the experimental data [see Fig. 1 (b)]. (ii) The density functional theory calculations suggest that in CaKFe$_4$As$_4$ ten bands (6 hole- and 4 electron-like bands) having different zero-temperature gap values cross the Fermi level.[45,46] Recent angle resolved photoemission (ARPES),[45] as well as the combination of ARPES and μSR experiments,[24] confirm this statement. This suggests, on the one hand, that the two-gap approach described by Eq. 2 is oversimplified and contributions of all ten bands need to be included. Such analysis requires, however, an exact knowledge of the electronic band structure.[24,47] On the other hand, similar two-gap approaches were previously used in Refs. 21,48,49 and allowed to describe satisfactorily the in-plane superfluid density data of CaKFe$_4$As$_4$. (iii) The difference in parameters obtained from the two-gap fit to $\lambda_{ab}^{-2}(T)$ and $\lambda_c^{-2}(T)$ are most probably caused by *anisotropic* contributions of various bands to the superfluid density. In such case Δ_1 and Δ_2 refer to averaged gaps for series of bands with 'big' and 'small' gap values, respectively (see *e.g.* Ref. 46), while ω correspond to the averaged weight of 'big' gaps to $\lambda^{-2}(0)$.

To conclude, the magnetic penetration depth anisotropy $\gamma_\lambda = \lambda_c/\lambda_{ab}$ in a CaKFe$_4$As$_4$ single crystal sample was studied by means of the muon-spin rotation. γ_λ is temperature independent for $T \lesssim 20$ K ($\gamma_\lambda \simeq 1.9$) and it increases up to $\gamma_\lambda \simeq 3.0$ for $T \to T_c$. The change of γ_λ induces the flux line lattice rearrangement, which is clearly detected via the enhanced distortions of FLL μSR response. The anisotropic properties of λ are explained by the multi-gap nature of superconductivity in CKaFe$_4$As$_4$ and caused by anisotropic contributions of various band to the in-plane and the out-of-plane components of the superfluid density.

* Electronic address: rustem.khasanov@psi.ch

[1] V.L. Ginzburg and L.D. Landau, Zh. Eksp. Teor. Fiz. **20**, 1064 (1950).

[2] V.L. Ginzburg, Zh. Eksp. Teor. Fiz. **23**, 236 (1952).

[3] C. Caroli, P. G. De Gennes, and J. Matricon, Phys. Konden. Mater. **1**, 176 (1963).

[4] S.L. Thiemann, Z. Radović, and V.G. Kogan, Phys. Rev. B **39**, 11406 (1989).

[5] M. Tinkham, *Introduction to Superconductivity* (Krieger Publishing company, Malabar, Florida, 1975).

[6] L.P. Gorkov and T.K. Melik-Barkhudarov, Sov. Phys. JETP **18**, 1031 (1964).

[7] V.G. Kogan, Phys. Rev. Lett. **89**, 237005 (2002).

[8] M. Angst, R. Puzniak, A. Wisniewski, J. Jun, S. M. Kazakov, J. Karpinski, J. Roos, and H. Keller, Phys. Rev. Lett. **88**, 167004 (2002).

[9] M. Angst and R. Puzniak, in Focus on Superconductivity, ed. B.P. Martines, Vol. 1 (Nova Science Publishers, New York, 2004) (pp. 1-49).

[10] J.D. Fletcher, A. Carrington, O. J. Taylor, S. M. Kazakov, and J. Karpinski Phys. Rev. Lett. **95**, 097005 (2005).

[11] R. Khasanov, A. Shengelaya, A. Bussmann-Holder, J. Karpinski, H. Keller, K. A. Müller, J. Supercond. Nov. Magn **21**, 1557 (2008).

[12] R. Khasanov, S. Strässle, D. Di Castro, T. Masui, S. Miyasaka, S. Tajima, A. Bussmann-Holder, and H. Keller, Phys. Rev. Lett. 99, 237601 (2007).

[13] R. Prozorov, M. A. Tanatar, R. T. Gordon, C. Martin, H. Kim, V. G. Kogan, N. Ni, M. E. Tillman, S. L. Bud'ko, P. C. Canfield, Physica C **469**, 582-589 (2009).

[14] R. Khasanov, D. V. Evtushinsky, A. Amato, H.-H. Klauss, H. Luetkens, Ch. Niedermayer, B. Büchner, G. L. Sun, C. T. Lin, J. T. Park, D. S. Inosov, and V. Hinkov, Phys. Rev. Lett. **102**, 187005 (2009).

[15] R. Khasanov, A. Maisuradze, H. Maeter, A. Kwadrin, H. Luetkens, A. Amato, W. Schnelle, H. Rosner, A. Leithe-Jasper, and H.-H. Klauss, Phys. Rev. Lett. **103**, 067010 (2009).

[16] S. Weyeneth, R. Puzniak, N. D. Zhigadlo, S. Katrych, Z. Bukowski, J. Karpinski, and H. Keller, J. Supercond. Nov. Magn. **22**, 347 (2009).

[17] S. Weyeneth, R. Puzniak, U. Mosele, N. D. Zhigadlo, S. Katrych, Z. Bukowski, J. Karpinski, S. Kohout, J. Roos, and H. Keller, J. Supercond. Nov. Magn. **22**, 325 (2009).

[18] M. Bendele, S. Weyeneth, R. Puzniak, A. Maisuradze, E. Pomjakushina, K. Conder, V. Pomjakushin, H. Luetkens, S. Katrych, A. Wiesniewski, R. Khasanov, and H. Keller, Phys. Rev. B **81**, 224520 (2010).

[19] S.O. Katterwe, Th. Jacobs, A. Maljuk, and V.M. Krasnov, Phys. Rev. B **89**, 214516 (2014).

[20] See Supplemental Information at http://link.aps.org/supplemental/xxxxx for description of the experimental techniques and the data analysis procedure, which includes Refs. 50,51,51,53–58.

[21] W.R. Meier, T. Kong, U.S. Kaluarachchi, V. Taufour, N.H. Jo, G. Drachuck, A.E. Böhmer, S.M. Saunders, A. Sapkota, A. Kreyssig, M.A. Tanatar, R. Prozorov, A.I. Goldman, F.F. Balakirev, A. Gurevich, S.L. Bud'ko, and P. C.

[21] Canfield, Phys. Rev. B **94**, 064501 (2016).

[22] W.R. Meier, T. Kong, S.L. Bud'ko, and P.C. Canfield, Phys. Rev. Materials **1**, 013401 (2017).

[23] A. Amato, H. Luetkens, K. Sedlak, A. Stoykov, R. Scheuermann, M. Elender, A. Raselli, and D. Graf, Review of Scientific Instruments **88**, 093301 (2017).

[24] R. Khasanov, W.R. Meier, Y. Wu, D. Mou, S.L. Bud'ko, I. Eremin, H. Luetkens, A. Kaminski, P.C. Canfield, and A. Amato, Phys. Rev. B 97, 140503(R) (2018).

[25] R. Khasanov, H. Zhou, A. Amato, Z. Guguchia, E. Morenzoni, X. Dong, G. Zhang, and Z.-X. Zhao Phys. Rev. B **93**, 224512 (2016).

[26] A. Suter and B. M. Wojek, Phys. Procedia **30**, 69 (2012).

[27] In $B_{ex} \parallel c$ experiments, the external field $B_{ex} = 10.8$ mT is applied perpendicular to the flat surface of the sample. Due to big demagnetization effects in such geometry (the demagnetization factor $N \simeq 0.98$, Ref. 59) the vortex lattice forms at fields higher than $\mu_0 H_{c1}^{\parallel c}(0) \cdot (1-N) \simeq 0.4$ mT $[\mu_0 H_{c1}^{\parallel c}(0) \simeq 20.8$ mT, Ref. 20]. In $B_{ex} \parallel ab$ experiments, $B_{ex} = 10.8$ mT is slightly smaller than $\mu_0 H_{c1}^{\parallel ab}(0) \simeq 12.2$ mT.[20] However, due the presence of a strong pinning in CaKFe$_4$As$_4$,[30,31] the 'rigid' FLL sets in slightly below T_c, where $B_{ex} \gg \mu_0 H_{c1}^{\parallel ab}(T \simeq T_c) \simeq 0$, and remains unchanged by further cooling down the sample.

[28] J.E. Sonier, R.F. Kiefl, J.H. Brewer, D.A. Bonn, J.F. Carolan, K.H. Chow, P.Dosanjh, W.N. Hardy, R. Liang, W.A. MacFarlane, P. Mendels, G.D. Morris, T.M. Riseman, and J.W. Schneider, Phys. Rev. Lett. **72**, 744 (1994).

[29] A. Maisuradze, R. Khasanov, A. Shengelaya, and H. Keller, J. Phys.: Condens. Matter **21**, 075701 (2009).

[30] A. Fente, W.R. Meier, T. Kong, V.G. Kogan, S.L. Bud'ko, P.C. Canfield, I. Guillamn, and H. Suderow, Phys. Rev. B **97**, 134501 (2018).

[31] S.J. Singh, M. Bristow, W.R. Meier, P. Taylor, S.J. Blundell, P.C. Canfield, and A.I. Coldea, Phys. Rev. Materials **2**, 074802 (2018).

[32] M. Weber, A. Amato, F. N. Gygax, A. Schenck, H. Maletta, V. N. Duginov, V. G. Grebinnik, A. B. Lazarev, V. G. Olshevsky, V. Yu. Pomjakushin, S. N. Shilov, V. A. Zhukov, B. F. Kirillov, A. V. Pirogov, A. N. Ponamarev, V. G. Storchak, S. Kapusta, and J. Bock, Phys. Rev. B **48**, 13022 (1993).

[33] E. H. Brandt, Phys. Rev. B **37**, 2349(R) (1988).

[34] E. H. Brandt, Phys. Rev. B **68**, 054506 (2003).

[35] C. M. Aegerter, J. Hofer, I. M. Savić, H. Keller, S. L. Lee, C. Ager, S. H. Lloyd, and E. M. Forgan Phys. Rev. B 57, 1253 (1998).

[36] S. L. Lee, P. Zimmermann, H. Keller, M. Warden, I. M. Savić, R. Schauwecker, D. Zech, R. Cubitt, E. M. Forgan, P. H. Kes, T. W. Li, A. A. Menovsky, and Z. Tarnawski, Phys. Rev. Lett. **71**, 3862 (1993).

[37] T. Blasius, Ch. Niedermayer, J. L. Tallon, D. M. Pooke, A. Golnik, and C. Bernhard, Phys. Rev. Lett. **82**, 4926 (1999).

[38] G. I. Menon, A. Drew, U. K. Divakar, S. L. Lee, R. Gilardi, J. Mesot, F. Y. Ogrin, D. Charalambous, E. M. Forgan, N. Momono, M. Oda, C. Dewhurst, and C. Baines, Phys. Rev. Lett. 97, 177004 (2006).

[39] R. Khasanov, Takeshi Kondo, S. Strässle, D.O.G. Heron, A. Kaminski, H. Keller, S. L. Lee, and T. Takeuchi, Phys. Rev. Lett. **101**, 227002 (2008)

[40] D.O.G. Heron, S. J. Ray, S. J. Lister, C. M. Aegerter, H. Keller, P. H. Kes, G. I. Menon, and S. L. Lee, Phys. Rev. Lett. **110**, 107004 (2013).

[41] A. Carrington and F. Manzano, Physica C **385**, 205 (2003).

[42] A.A. Golubov and A.E. Koshelev, Phys. Rev. B **68**, 104503 (2003).

[43] P. Miranović, K. Machida, and V.G. Kogan, J. Phys. Soc. Jpn. **72**,221 (2003).

[44] H. Padamsee, and J. E. Neighbor, and C. A. Shiffman, J. Low Temp. Phys. **12**, 387 (1973).

[45] D. Mou, T. Kong,W. R. Meier, F. Lochner, L.-L.Wang, Q. Lin, Y. Wu, S. L. Bud'ko, I. Eremin, D. D. Johnson, P. C. Canfield, and A. Kaminski, Phys. Rev. Lett. **117**, 277001 (2016).

[46] F. Lochner, F. Ahn, T. Hickel, and I. Eremin, Phys. Rev. B **96**, 094521 (2017).

[47] D.V. Evtushinsky, D.S. Inosov, V.B. Zabolotnyy, M.S. Viazovska, R. Khasanov, A. Amato, H.-H. Klauss, H. Luetkens, Ch. Niedermayer, G.L. Sun, V. Hinkov, C.T. Lin, A. Varykhalov, A. Koitzsch, M. Knupfer, B. Büchner, A.A. Kordyuk, and S.V. Borisenko, New Journal of Physics, **11**, 055069 (2009).

[48] K. Cho, A. Fente, S. Teknowijoyo, M. A. Tanatar, K. R. Joshi, N. M. Nusran, T. Kong, W. R. Meier, U. Kaluarachchi, I. Guillamón, H. Suderow, S. L. Bud'ko, P. C. Canfield, and R. Prozorov, Phys. Rev. B **95**, 100502(R)

[49] (2017).

[49] P. K. Biswas, A. Iyo, Y. Yoshida, H. Eisaki, K. Kawashima, and A. D. Hillier, Phys. Rev. B **95**, 140505(R) (2017).

[50] J.E. Sonier, K.F. Poon, G.M. Luke, P. Kyriakou, R.I. Miller, R. Liang, C.R. Wiebe, P. Fournier, and R.L. Greene, Phys. Rev. Lett. **91**, 147002 (2003).

[51] R. Khasanov, K. Conder, E. Pomjakushina, A. Amato, C. Baines, Z. Bukowski, J. Karpinski, S. Katrych, H.-H. Klauss, H. Luetkens, A. Shengelaya, and N. D. Zhigadlo, Phys. Rev. B **78**, 220510(R) (2008).

[52] R. Khasanov, H. Luetkens, A. Amato, H.-H. Klauss, Z.-A. Ren, J. Yang, W. Lu, and Z.-X. Zhao, Phys. Rev. B **78**, 092506 (2008).

[53] R. Khasanov, D. G. Eshchenko, D. Di Castro, A. Shengelaya, F. La Mattina, A. Maisuradze, C. Baines, H. Luetkens, J. Karpinski, S. M. Kazakov, and H. Keller, Phys. Rev. B **72**, 104504 (2005).

[54] A. Yaouanc, P. Dalmas de Réotier, and E. H. Brandt, Phys. Rev. B **55**, 11107 (1997).

[55] E.H. Brandt, J. Low Temp. Phys. **26**, 709 (1977).

[56] E.H. Brandt, J. Low Temp. Phys. **73**, 355 (1988).

[57] J. Rammer, Physica C **177**, 421 (1991).

[58] T.M. Riseman, J.H. Brewer, K.H. Chow, W.N. Hardy, R.F. Kiefl, S.R. Kreitzman, R. Liang, W.A. MacFarlane, P. Mendels, G.D. Morris, J. Rammer, J.W. Schneider, C. Niedermayer, and S.L. Lee, Phys. Rev. B **52**, 10569 (1995).

[59] R. Prozorov and V. G. Kogan, Phys. Rev. Applied **10**, 014030 (2018).